

Geometry, electronic structure, and optical properties of boron cages: A first-principles DFT study

Kashinath T. Chavan,^{*,†} Ihsan Boustani,^{*,‡} and Alok Shukla^{*,†}

[†]*Department of Physics, Indian Institute of Technology Bombay, Mumbai 400076, India.*

[‡]*Theoretical and Computational Chemistry, Faculty of Mathematics and Natural Sciences, Bergische Universität Wuppertal, D-42097 Wuppertal, Germany.*

E-mail: ktchavan99@gmail.com; ifboustani@gmail.com; shukla@iitb.ac.in

Abstract

A systematic study of the structural, electronic, and optical properties of cage-like boron clusters, with the number of constituent atoms ranging from 20 to 122, has been carried out within the framework of density-functional theory (DFT), employing 6-31G(d, p) extended basis set. The dynamic stability of the clusters is analyzed through the vibrational frequency analysis, while to study the thermodynamic stability, we computed their binding energies per atom. The results suggest that the 32- and 92-atom cages are the most stable among the small and the large structures. The optical absorption spectra of these cages is computed using the time-dependent density-functional theory (TDDFT), which suggests their applications in optoelectronic devices in the visible range of the spectrum.

Introduction

In the era of nanotechnology, researchers continue to seek increasingly efficient materials and their nano-structural forms for the technological applications.¹ Among the various nano-structural forms, cage-like atomic clusters are particularly notable due to their unique properties and tunability which suggest that they could play a crucial role in the next-generation devices. Boron, due to its neutron-absorbing properties, is a key element with applications in cancer treatment and nuclear reactors. The carbides, hydrides, oxides, and nitrides of boron have a wide range of applications such as hydrogen storage, high energy fuels, anticorrosive coatings, photocatalysts, etc.²⁻⁷ Boron nanostructures have wide-ranging applications in a variety of fields such as drug design,⁸ and hydrogen storage.⁹⁻¹² Boron, as a neighbor of carbon in the periodic table with single electron in the p orbital, draws the attention on its nanostructures. Just as graphene evolved from fullerenes to nanotubes to single atomic sheets, there is high interest in the potential unfolding of boron, particularly following the prediction of the B_{80} cage cluster.¹³⁻¹⁵ The smaller-sized boron clusters tend to acquire a planer geometry, while the larger ones stabilize in spherical structures.¹⁶⁻¹⁹ Among the spherical cage structures, the core shell type cages where B_{12} is the core cluster, are predicted to be thermodynamically more stable than the hollow ones.²⁰ These cage clusters constitutes as a super-atom in the self-assembled nanostructures.^{21,22} The properties of boron cage-like cluster and their self-assemblies can be tuned to the desired extent by exohedral and endohedral doping of impurity atom,²³⁻²⁵ for example, a magnetic impurity atom that results in the large spin polarization which could be utilized for the spintronics.²⁶ The boron compounds and its nanostructures have the excellent optical properties,^{7,27-30} however, its atomic clusters are yet to adequately explored for their optical properties.³¹ The the first principles method, the time dependent density functional theory (TDDFT) within a accurate basis set provides the description of excited states of the nanostructures that can be compared with the experiments. On this ground, it would be valuable to systematically investigate the optical properties of boron clusters using accurate basis sets, in light of their potential

applicability in the optoelectronic devices.

In the present study, we investigate cage-like boron cluster with the number of constituent atoms ranging from 20 to 122, and discuss their geometry, stability, electronic structure, and the optical properties.

Computational details

The calculations for geometry optimization and the optical absorption spectra for the cage-like atomic clusters of the boron are carried out using the Gaussian16 code,³² and 6-31G(d, p) extended basis set. The clusters, along with their isomers, contain 20, 32, 42, 60, 72, 80, 92, 100, 110, and 122 boron atoms. The Benny algorithm was used for geometry optimization and the convergence thresholds for maximum force on an atom, and the RMS force were set at 0.023 eV/Å, and 0.015 eV/Å, respectively. The relaxed cages exhibit a variety of structures such as dodecahedron (B₂₀), icosahedron (B₉₂, B₁₁₀), convex (B₈₀, B₉₂), d5h (B₂₀), fullerene (B₈₀), etc. For the relaxed structures, the optical absorption spectra (OAS) has been studied within the TDDFT as implemented in the Gaussian code.³² The B3LYP as hybrid exchange-correlation functional and the 6-31G(d, p) as the localized basis set have been used for this purpose. For the self-consistent-field calculations, the energy convergence criterion is set to 0.0002 eV. The GaussView utility is used for the extraction the output data.³³ Unless mentioned otherwise, the structures studied are charge neutral and in spin singlet state, and the OAS is calculated for the first 60 excited states in all the cases. To analyze the thermodynamic stability of these clusters, we compute their binding energy per atom (B.E.) using the formula.

$$B.E. = \frac{N \times E(B) - E(B_N)}{N},$$

where N is the number of boron atoms in the cage, $E(B)$ is the total energy of an isolated boron atom, and $E(B_N)$ is the total energy of the cage. The total energy of the isolated boron atom obtained from the SCF calculations is -670.88 eV, used for the binding energy

calculations.

Results and discussion

To obtain the stable structure for the given configuration, the initial geometries of clusters are relaxed to local minima on the potential energy surface. The final optimized geometries of boron cage clusters are shown in the Figure 1. It is observed in most of the cases that the clusters retain their cage-like geometry with the exception of the B_{42} cluster, which gets distorted.

The B_{20} cage has two isomers, the first one with D_{5h} symmetry, while the second one with the dodecahedral symmetry. In D_{5h} case, the structure has overlapping pentagons with non-uniform inter-pentagon separations, whereas, dodecahedron has a ring-like top view due to non-overlapping pentagons with a uniform inter-pentagon separation of 2.65 Å. The intra-pentagon B-B bond length is 1.66 Å. The sizes of the clusters in D_{5h} and dodecahedron isomer are 5.47 Å and 4.89 Å, respectively. However, their bond-length range (1.62-1.83 Å) and binding energies (4.69, 4.66 eV) are substantially close. In the electronic structure, the HOMO-LUMO (H-L) gap is larger in dodecahedron (2.47 eV) than that in D_{5h} (1.51 eV). However, both of these isomers are dynamically unstable as learned from the vibrational frequencies.

The B_{32} is the cluster with the largest H-L gap (2.44 eV) that is dynamically stable. This is qualitatively consistent with the earlier report.³⁴ The B_{32} structure was created by placing the boron atoms at the center of each 12 pentagons and 20 hexagons of C_{60} . The size of the optimized structure is 5.44 Å, and its bond length varies between 1.63 Å to 1.78 Å. The final B_{32} cluster has eight hexagons with atoms at their center and six squares. The binding energy per atom of the B_{32} cluster is 4.83 eV. Based on its symmetry, H-L gap, and binding energies, this cluster could be explored for the optoelectronic device applications.

The B_{42} cluster does not retain its initial structural symmetry upon relaxation and undergoes

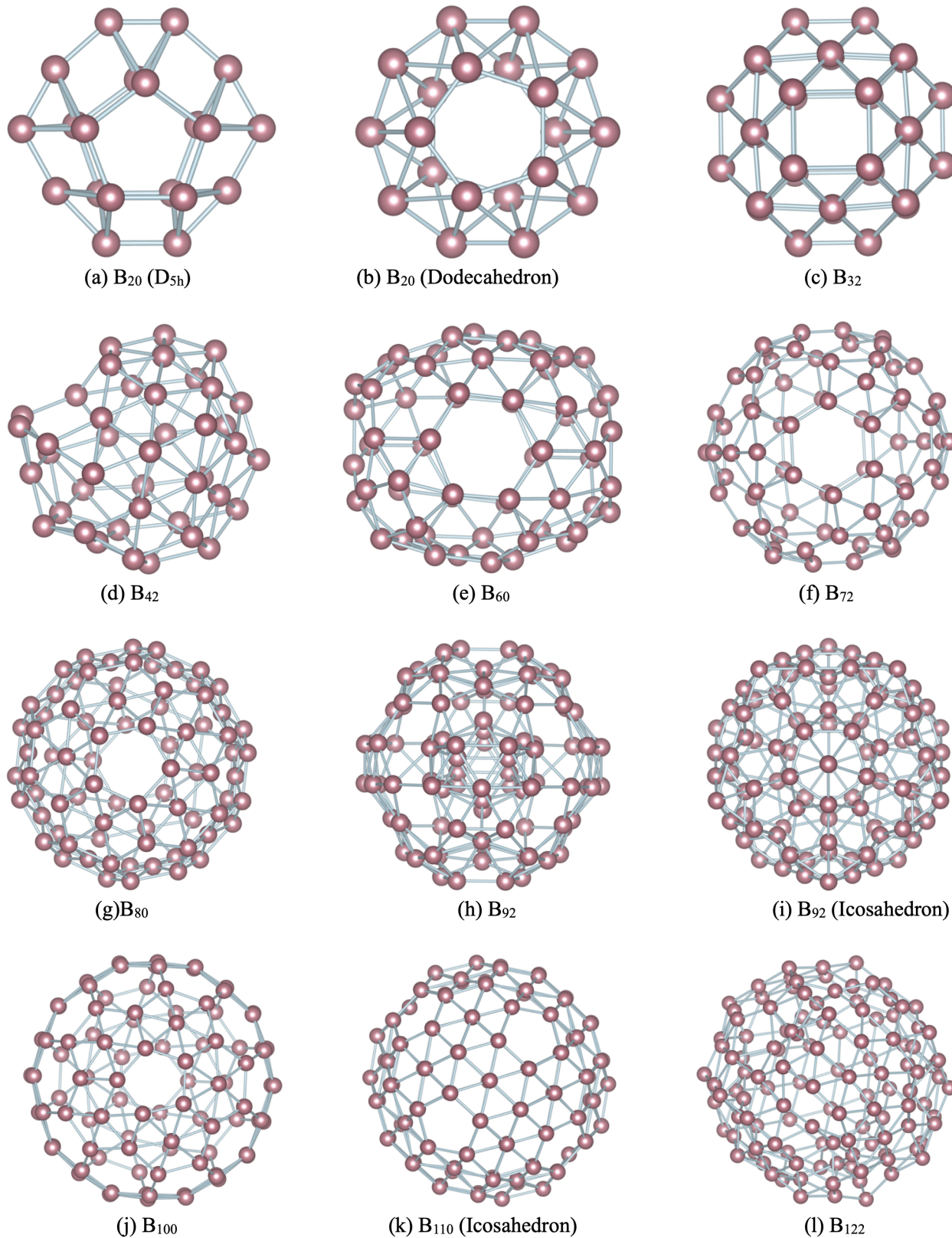


Figure 1: The optimized geometries of the boron cage-like clusters, B_N , where N denotes the number of constituting boron atoms. The structures are either hollow or encapsulated cages.

distortions, however, the final structure has some hollow space within it, and can be identified as a cage. The per atom binding energy of this structure is 5.0 eV, and the H-L gap is 2.0 eV. Its bond lengths lie in the range of 1.54 Å-1.73 Å with cluster size, 6.75 Å.

The B₆₀ cluster is elongated sphere and that looks like a barrel-shape structure with septagon at its openings on each side. The size of the cluster is 8.41 Å, and its per atom binding energy is 5.15 eV which happens to be the largest among the dynamically stable clusters. The H-L gap is 1.57 eV and the bond lengths lie in the range 1.58 Å-1.77 Å.

The boron clusters B₂₀, B₃₂, B₄₂, B₆₀, atoms have different shapes but for the B₇₂ and beyond, the clusters stabilize in the spherical shape. Their surfaces are combinations of pentagons and hexagons with and without a atom at their centre.

The B₇₂ cluster comprises of pentagons, hexagons such that the five hexagons around each pentagon shares a side. Pentagons have atoms at the center, which are the vertices of this spherical-shaped cage, whereas the hexagons are planer. The B₇₂ has a diameter of 9.0 Å, and its bond lengths lie in the range of 1.60 Å-1.84 Å. The per atom binding energy is 5.10 eV, and the energy gap is 0.72 eV. Moreover, this cluster is dynamically stable.

In B₈₀, the structure is similar to that of B₇₂, except that pentagons are hollow, and hexagons have atoms at the center. Its diameter is 8.48 Å, and bond lengths in the range 1.66 Å-1.74 Å. B₈₀ has a per atom binding energy of 5.17 eV and an H-L gap of 1.94 eV. However, this B₈₀ cluster is dynamically unstable because during the vibrational frequency analysis we obtained seven imaginary frequencies.

In B₉₂, two isomers have been studied, convex and icosahedron. The convex structure is a B₈₀ cluster embedded with a B₁₂ cluster. We note that the six surface atoms which were at the centre of hexagons, have moved inward forming bonds with the embedded cluster. The icosahedron comprises triangles that host the hexagons on the surface; the center atom in all hexagons has moved inward. The convex structure has a size of 8.82 Å, while the icosahedron has 9.67 Å. The icosahedral structure is dynamically stable, with an almost double H-L gap (2.07 eV) compared to the convex case. The range of bond lengths for the convex case is

1.67 Å-1.84 Å, and for icosahedron, it is 1.63 Å-1.79 Å. The per atom binding energy of the convex structure (5.15 eV) is slightly higher than that of the icosahedron (5.10 eV).

B₁₀₀ cage has twelve pentagons, ten hexagons in hollow form and eighteen hexagons with an atom at their center. It can be viewed as three continuous strips of hexagons separated by hollow pentagons and hexagons. It has hollow pentagons at both poles. The cage has the most significant per atom binding energy, i.e., 5.18 eV, the smallest H-L gap, 0.60 eV, and is dynamically unstable as it has one vibrational mode with imaginary frequency. The size of this cage is 9.74 Å, and bond lengths lies in the range of 1.65 Å-1.77 Å.

In B₁₁₀ convex structure, the hollow pentagon is surrounded by five hexagons with atoms at their center. Its size is 9.89 Å and the bond length range is 1.67 Å-1.76 Å. The per atom binding energy of this cage is 5.10 eV with an H-L energy gap of 0.76 eV.

The B₁₂₂ is the largest cluster studied in this report, with a size extending up to 10.95 Å. It's per atom binding energy is 5.12 eV, and the H-L gap is 0.89 eV. The bond lengths lie in the range 1.58 Å- 1.84 Å, and the structure is dynamically stable. The energetics and structural details of these clusters are given in Table 1.

Table 1: The size (diameter), range of bond-lengths, HOMO-LUMO (H-L) gap, optical gap, per atom binding energies, and the dynamic stability of boron clusters. The multiple optical gaps refers to the shoulder and the principle peak in the optical absorption spectra. The dynamic stability based on vibrational analysis is termed as stable (Y) or unstable (N).

Cluster	Size (Å)	Bond length range (Å)	H-L gap (eV)	Optical gap (eV)	Binding energy (eV)/Atom	Dynamic Stability
B ₂₀	5.47	1.6-1.8	1.51	3.50	4.69	N
B ₂₀ (Dodecahedron)	4.89	1.66-1.83	2.47	2.29, 3.79	4.66	N
B ₃₂	5.44	1.63-1.78	2.44	2.59	4.83	Y
B ₄₂	6.75	1.54-1.73	2.00	2.60, 3.38	5.01	Y
B ₆₀	8.41	1.58-1.77	1.57	2.41	5.15	Y
B ₇₂	9.0	1.60-1.84	0.72	1.43	5.10	Y
B ₈₀	8.48	1.66-1.74	1.94	1.99	5.17	N
B ₉₂	8.82	1.67-1.84	0.99	0.90, 1.80	5.15	N
B ₉₂ (Icosahedron)	9.67	1.63-1.79	2.07	1.60	5.10	Y
B ₁₀₀	9.74	1.65-1.77	0.60	1.10	5.18	N
B ₁₁₀	9.89	1.67-1.76	0.76	1.15	5.10	N
B ₁₂₂	10.95	1.58-1.84	0.89	1.29	5.12	Y

Figure 2 shows the OAS for the above discussed boron clusters. Significant absorption is observed for the incident photon energy up to 7.0 eV. Often it is seen that the multiple excitations are responsible for the peaks in the OAS. However, we have considered and listed here those with significant oscillator strengths (> 0.002) and largest coefficient for a given energy.

The B₂₀ cluster's OAS has contributions from the three energy regions. The first peak is a minor shoulder around 1.8 eV, which is due to $|H-2 \rightarrow L\rangle$ excitation, where H (L) stands for HOMO (LUMO). The second peak is the moderate shoulder observed around 2.7 eV and has maximum contribution from the excitations, $|H-2 \rightarrow L+1\rangle$ and $|H-6 \rightarrow L+1\rangle$. The third one, which is the principal peak, occurs around 3.5 eV, with multiple electronic excitations such as $|H-1 \rightarrow L+2\rangle$, $|H-8 \rightarrow L+1\rangle$, $|H \rightarrow L+5\rangle$, $|H \rightarrow L+5\rangle$, $|H-3 \rightarrow L+3\rangle$, and $|H-4 \rightarrow L+3\rangle$ contributing to it. The other isomer of B₂₀ studied has a dodecahedron structure.

Among the B₂₀ cages, the amplitude of optical absorption for dodecahedron case is higher by an order of magnitude. It has two peaks in its optical absorption, a minor shoulder peak at

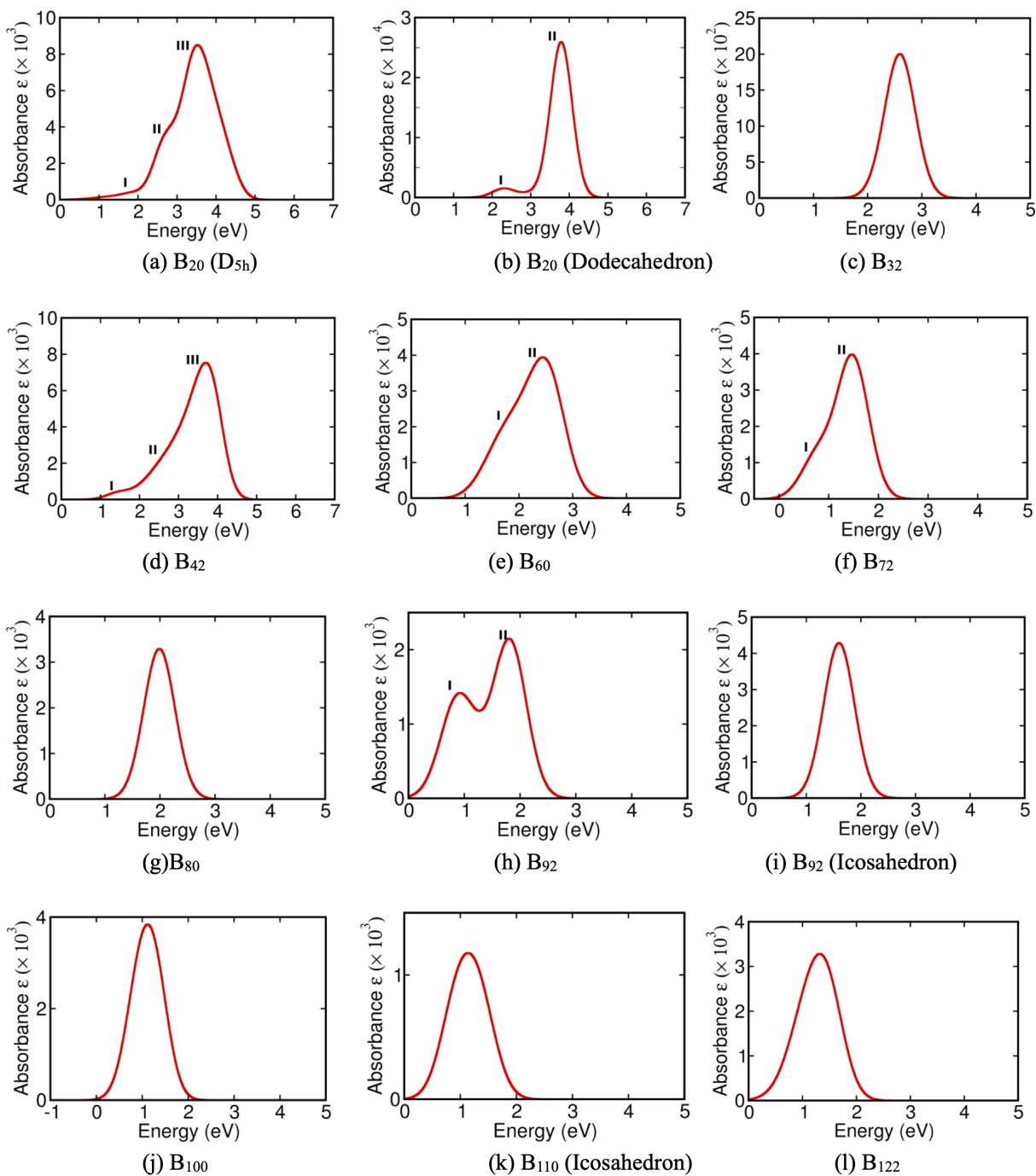


Figure 2: The linear optical absorption spectra of boron clusters computed using TDDFT approach, at the 6-31G(d,p)/B3LYP level of theory.

2.3 eV and a quite intense one at energy 3.8 eV. The excitations corresponding to the small peak are $|H-4 \rightarrow L\rangle$, $|H-4 \rightarrow L+1\rangle$, whereas for the intense peak, that are $|H-1 \rightarrow L+3\rangle$, $|H-3 \rightarrow L+4\rangle$, and $|H \rightarrow L+5\rangle$.

The B_{32} cluster has a single peak at 2.59 eV in its absorption spectrum with the least intensity among all the clusters. The excitations correspond to this peak are $|H-1 \rightarrow L+3\rangle$, $|H-2 \rightarrow L+3\rangle$, and $|H-2 \rightarrow L+4\rangle$ and these excitations have equal oscillator strengths. The B_{42} cluster, with a distorted structure, has two shoulders (I and II) located at 1.2 eV and 2.4 eV, and a major peak (III) at 3.8 eV in its OAS, and the excitations contributing to them are listed in the Supporting Information (SI). The OAS of B_{60} has a shoulder (I) at 1.8 eV, and an intense peak (II) at 2.6 eV. The excitations contributing to I are $|H-2 \rightarrow L\rangle$, $|H-4 \rightarrow L\rangle$, $|H-2 \rightarrow L+2\rangle$, $|H-2 \rightarrow L+3\rangle$, $|H-4 \rightarrow L+2\rangle$, and $|H-4 \rightarrow L+3\rangle$, whereas, those to II are $|H \rightarrow L+5\rangle$, $|H-7 \rightarrow L\rangle$, $|H-1 \rightarrow L+3\rangle$, $|H-2 \rightarrow L+4\rangle$, $|H \rightarrow L+6\rangle$, $|H-3 \rightarrow L+3\rangle$, $|H-7 \rightarrow L+1\rangle$, $|H-3 \rightarrow L+5\rangle$, $|H-1 \rightarrow L+6\rangle$, $|H \rightarrow L+8\rangle$, $|H-3 \rightarrow L+6\rangle$, $|H-10 \rightarrow L\rangle$, and $|H-10 \rightarrow L\rangle$. In B_{72} , the optical absorption spectrum is similar to B_{60} , except the absorption edge of B_{72} is at a relatively lower energy. Its first peak which is shoulder located 0.79 eV is due to the excitations, $|H-2 \rightarrow L\rangle$, $|H-2 \rightarrow L+1\rangle$, $|H-5 \rightarrow L\rangle$, $|H-4 \rightarrow L+2\rangle$, and $|H-5 \rightarrow L+2\rangle$. The peak is at around 1.54 eV, and the excitations responsible are $|H-3 \rightarrow L+5\rangle$, $|H-3 \rightarrow L+6\rangle$, $|H-2 \rightarrow L+4\rangle$, $|H-4 \rightarrow L+3\rangle$, $|H-5 \rightarrow L+3\rangle$, $|H-4 \rightarrow L+4\rangle$, $|H-5 \rightarrow L+5\rangle$, $|H-5 \rightarrow L+5\rangle$, $|H-1 \rightarrow L+7\rangle$, and $|H-1 \rightarrow L+10\rangle$. The B_{80} cluster has a single peak in the OAS at energy 1.99 eV due to a single transition; $|H-4 \rightarrow L+3\rangle$. In the B_{92} convex cluster, OAS has two clear peaks at energies 0.8 eV and 1.8 eV. The excitations responsible are $|H-3 \rightarrow L\rangle$, $|H-5 \rightarrow L\rangle$, $|H \rightarrow L+1\rangle$, and $|H-2 \rightarrow L+6\rangle$, $|H-3 \rightarrow L+6\rangle$, $|H-4 \rightarrow L+3\rangle$, $|H-4 \rightarrow L+5\rangle$, respectively. In contrast to the B_{92} convex cage, the B_{92} icosahedron has only one peak at 1.6 eV with doubled intensity compared to that of the convex case. The excitations corresponding to this peak are $|H-2 \rightarrow L\rangle$, $|H-1 \rightarrow L+1\rangle$, and $|H \rightarrow L+3\rangle$. The B_{100} cluster's OAS also has a peak around 1.00 eV, and the corresponding transitions are $|H-4 \rightarrow L+3\rangle$, $|H-4 \rightarrow L+3\rangle$, $|H \rightarrow L+4\rangle$, $|H-1 \rightarrow L+5\rangle$, $|H-2 \rightarrow L+5\rangle$, and $|H-10 \rightarrow L+3\rangle$. Similarly, B_{110} also has a

single peak in the OAS at energy 1.3 eV, and the transitions responsible for this peak are $|H \rightarrow L+3\rangle$, $|H \rightarrow L+4\rangle$, $|H-1 \rightarrow L+4\rangle$, $|H-1 \rightarrow L+6\rangle$, $|H-1 \rightarrow L+5\rangle$, and $|H-1 \rightarrow L+9\rangle$. In the B_{122} case, the peak is around energy 1.3 eV, to which a large number of excitations listed in the SI contribute. The excitation energies, their oscillator strengths, and excitations for the OAS of all the boron clusters are provided in the SI.

The binding energies per atom of these clusters are plotted in the figure 3. It increases from B_{12} to B_{60} , and beyond that it does not change significantly. For B_{12} , it is close to 4.4 eV, and for the constant part, it is around 5.1 eV.

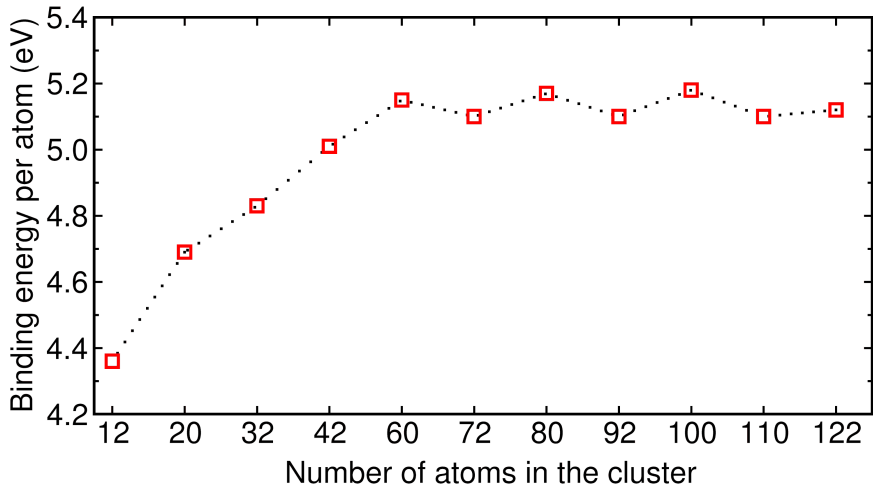


Figure 3: The binding energies per atom of the boron clusters. The dotted line is a guide to the eye.

Summary and conclusions

Boron cage-like clusters, ranging from 20 atoms with size 4.89 Å to 122 atoms with size 10.95 Å have been studied for structural and optical properties. The stabilities of these clusters through the vibrational frequencies and the per atom binding energies are discussed. The per atom binding energy of the cluster is observed to increase initially till B_{42} atom cluster and beyond that it remains nearly constant. The clusters B_{32} , B_{42} , B_{60} , B_{72} , B_{92} (Icosahedron), and B_{122} are found to be dynamically stable. Among the small clusters B_{32} is the most

stable one with the largest HOMO-LUMO gap whereas, among large clusters, B₉₂ is the most stable cluster. The optical gap for most of the clusters lies in the visible spectrum of light which suggests the potential application of these clusters in the optoelectronics. Since these clusters provides adequate space inside the cage for encapsulation or endohedral doping by an atom or molecule, it is of interest to manipulate the properties of clusters especially in light the optoelectronic and spintronics device applications.

Conflicts of interest

There are no conflicts to declare.

Acknowledgement

KTC acknowledges Arifa Nazir Bhat and Khushboo Dange, PhD scholars at IIT Bombay for technical discussions.

References

- (1) Zhang, H.; Li, J.; Yang, C.; Guo, X. Single-molecule functional chips: unveiling the full potential of molecular electronics and optoelectronics. *Accounts of Materials Research* **2024**, *5*, 971–986.
- (2) Kozień, D.; Szermer-Olearnik, B.; Rapak, A.; Szczygieł, A.; Anger-Góra, N.; Boratyński, J.; Pajtasz-Piasecka, E.; Bućko, M. M.; Pędzich, Z. Boron-rich boron carbide nanoparticles as a carrier in boron neutron capture therapy: Their influence on tumor and immune phagocytic cells. *Materials* **2021**, *14*, 3010.
- (3) Hagemann, H. Boron hydrogen compounds: hydrogen storage and battery applications. *Molecules* **2021**, *26*, 7425.

- (4) Han, L.; Wang, R.; Chen, W.; Wang, Z.; Zhu, X.; Huang, T. Preparation and combustion mechanism of boron-based high-energy fuels. *Catalysts* **2023**, *13*, 378.
- (5) Verma, C.; Dubey, S.; Barsoum, I.; Alfantazi, A.; Ebenso, E. E.; Quraishi, M. Hexagonal boron nitride as a cutting-edge 2D material for additive application in anticorrosive coatings: Recent progress, challenges and opportunities. *Materials Today Communications* **2023**, *35*, 106367.
- (6) Hayat, A.; Sohail, M.; Hamdy, M. S.; Taha, T.; AlSalem, H. S.; Alenad, A. M.; Amin, M. A.; Shah, R.; Palamanit, A.; Khan, J.; others Fabrication, characteristics, and applications of boron nitride and their composite nanomaterials. *Surfaces and Interfaces* **2022**, *29*, 101725.
- (7) Revabhai, P. M.; Singhal, R. K.; Basu, H.; Kailasa, S. K. Progress on boron nitride nanostructure materials: properties, synthesis and applications in hydrogen storage and analytical chemistry. *Journal of Nanostructure in Chemistry* **2023**, *13*, 1–41.
- (8) Lesnikowski, Z. J. Challenges and opportunities for the application of boron clusters in drug design. *Journal of medicinal chemistry* **2016**, *59*, 7738–7758.
- (9) Zhao, Y.; Lusk, M. T.; Dillon, A. C.; Heben, M. J.; Zhang, S. B. Boron-based organometallic nanostructures: hydrogen storage properties and structure stability. *Nano letters* **2008**, *8*, 157–161.
- (10) Wu, G.; Wang, J.; Zhang, X.; Zhu, L. Hydrogen storage on metal-coated B80 buckyballs with density functional theory. *The Journal of Physical Chemistry C* **2009**, *113*, 7052–7057.
- (11) Li, M.; Li, Y.; Zhou, Z.; Shen, P.; Chen, Z. Ca-coated boron fullerenes and nanotubes as superior hydrogen storage materials. *Nano letters* **2009**, *9*, 1944–1948.

- (12) Huang, Z.; Wang, S.; Dewhurst, R. D.; Ignat'ev, N. V.; Finze, M.; Braunschweig, H. Boron: its role in energy-related processes and applications. *Angewandte Chemie International Edition* **2020**, *59*, 8800–8816.
- (13) Gonzalez Szwacki, N.; Sadrzadeh, A.; Yakobson, B. I. B 80 fullerene: an ab initio prediction of geometry, stability, and electronic structure. *Physical review letters* **2007**, *98*, 166804.
- (14) Mishra, R. K.; Sarkar, J.; Verma, K.; Chianella, I.; Goel, S.; Nezhad, H. Y. Borophene: A 2D wonder shaping the future of nanotechnology and materials science. *Nano Materials Science* **2025**, *7*, 198–230.
- (15) Li, Q.; Kolluru, V. S. C.; Rahn, M. S.; Schwenker, E.; Li, S.; Hennig, R. G.; Darancet, P.; Chan, M. K.; Hersam, M. C. Synthesis of borophane polymorphs through hydrogenation of borophene. *Science* **2021**, *371*, 1143–1148.
- (16) Alexandrova, A. N.; Boldyrev, A. I.; Zhai, H.-J.; Wang, L.-S. All-boron aromatic clusters as potential new inorganic ligands and building blocks in chemistry. *Coordination Chemistry Reviews* **2006**, *250*, 2811–2866.
- (17) Huang, W.; Sergeeva, A. P.; Zhai, H.-J.; Averkiev, B. B.; Wang, L.-S.; Boldyrev, A. I. A concentric planar doubly π -aromatic B19- cluster. *Nature chemistry* **2010**, *2*, 202–206.
- (18) Zubarev, D. Y.; Boldyrev, A. I. Comprehensive analysis of chemical bonding in boron clusters. *Journal of computational chemistry* **2007**, *28*, 251–268.
- (19) Mukhopadhyay, S.; He, H.; Pandey, R.; Yap, Y. K.; Boustani, I. Novel spherical boron clusters and structural transition from 2D quasi-planar structures to 3D double-rings. *Journal of Physics: Conference Series*. 2009; p 012028.
- (20) Zhao, J.; Wang, L.; Li, F.; Chen, Z. B80 and other medium-sized boron clusters: core-

- shell structures, not hollow cages. *The Journal of Physical Chemistry A* **2010**, *114*, 9969–9972.
- (21) Liu, A. Y.; Zope, R. R.; Pederson, M. R. Structural and bonding properties of bcc-based B 80 solids. *Physical Review B—Condensed Matter and Materials Physics* **2008**, *78*, 155422.
- (22) Yan, Q.-B.; Zheng, Q.-R.; Su, G. Face-centered-cubic B 80 metal: Density functional theory calculations. *Physical Review B—Condensed Matter and Materials Physics* **2008**, *77*, 224106.
- (23) Jin, P.; Hao, C.; Gao, Z.; Zhang, S. B.; Chen, Z. Endohedral metalloborofullerenes La₂@ B₈₀ and Sc₃N@ B₈₀: a density functional theory prediction. *The Journal of Physical Chemistry A* **2009**, *113*, 11613–11618.
- (24) Li, J.; Yang, G. Ni@ B₈₀: a single molecular magnetic switch. *Applied Physics Letters* **2009**, *95*.
- (25) Yan, Q.-B.; Zheng, Q.-R.; Su, G. Face-centered-cubic K₃ B₈₀ and Mg₃ B₈₀ metals: Covalent and ionic bondings. *Physical Review B—Condensed Matter and Materials Physics* **2009**, *80*, 104111.
- (26) Chavan, K. T.; Chandra, S.; Kshirsagar, A. Tunnel barrier to spin filter: Electronic-transport characteristics of transition metal atom encapsulated in a small Cadmium Telluride cage. *Nanoscale* **2023**, *15*, 1327–1337.
- (27) Tian, Y.; Guo, Z.; Zhang, T.; Lin, H.; Li, Z.; Chen, J.; Deng, S.; Liu, F. Inorganic boron-based nanostructures: Synthesis, optoelectronic properties, and prospective applications. *Nanomaterials* **2019**, *9*, 538.
- (28) Yin, J.; Li, J.; Hang, Y.; Yu, J.; Tai, G.; Li, X.; Zhang, Z.; Guo, W. Boron nitride

- nanostructures: fabrication, functionalization and applications. *Small* **2016**, *12*, 2942–2968.
- (29) Moon, S.; Kim, J.; Park, J.; Im, S.; Kim, J.; Hwang, I.; Kim, J. K. Hexagonal boron nitride for next-generation photonics and electronics. *Advanced Materials* **2023**, *35*, 2204161.
- (30) Uddin, M. M.; Kabir, M. H.; Ali, M. A.; Hossain, M. M.; Khandaker, M. U.; Mandal, S.; Arifuzzaman, A.; Jana, D. Graphene-like emerging 2D materials: recent progress, challenges and future outlook. *RSC advances* **2023**, *13*, 33336–33375.
- (31) Bhattacharyya, P.; Boustani, I.; Shukla, A. First principles study of structural and optical properties of B12 isomers. *Journal of Physics and Chemistry of Solids* **2019**, *133*, 108–116.
- (32) Frisch, M. J. et al. Gaussian 16 Revision C. 01, 2016. *Gaussian Inc. Wallingford CT* **2016**, *1*, 572.
- (33) Dennington, R.; Keith, T. A.; Millam, J. M.; others GaussView 6.0. 16. *Semichem Inc.: Shawnee Mission, KS, USA* **2016**, 143–150.
- (34) Sheng, X.-L.; Yan, Q.-B.; Zheng, Q.-R.; Su, G. Boron fullerenes B₃₂+ 8k with four-membered rings and B₃₂ solid phases: geometrical structures and electronic properties. *Physical Chemistry Chemical Physics* **2009**, *11*, 9696–9702.

TOC Graphic

